We thank the referee for the insightful comments. Below, we repeat the reviewer's remarks in red italics, and add our respective responses in normal text.

Reviewer 1

General comments

This study assesses the Northern Hemisphere stratospheric polar vortex response to localized gravity wave forcing above three hotspot regions, the Himalayas, Northwest America, and East Asia, using UA-ICON GCM. The results highlight that all hotspot forcings consistently reduce planetary wave 1 amplitude, which is discussed in detail. I find the study highly relevant, especially due to the classification framework developed and its application to transient climate simulations and reanalyses. I recommend publication once the minor comments below are addressed.

We sincerely thank the reviewer for the thoughtful evaluation and positive feedback on our study. We appreciate the reviewer's valuable comments, which have helped improve the scientific clarity and overall quality of the manuscript.

Specific comments

I noticed that in Fig. 6 in Mehrdad (2025a), the zonal-mean climatology of the tendencies induced by the OGW parameterization scheme shows a secondary maximum in the lower stratosphere over midlatitudes, within the so-called valve layer (Kruse et al., 2016). However, this maximum is located around and below 100 hPa. This contrasts with the breaking of freely propagating OGWs above the center of the UTLS jet starting rather above in CMIP6 AMIP simulations (Hajkova and Sacha, 2024). Can you comment on this deficiency or model tuning with respect to vertical profiles of OGWD in the sensitivity simulations above NA and HI, where the breaking is maximized below 100 hPa (see Fig. 3 in Mehrdad (2025a))? This can consequently affect the polar vortex response simulated by UA-ICON.

We thank the reviewer for the insightful comment emphasizing the importance of the model's climatological vertical distribution of subgrid-scale orographic (SSO) gravity-wave (GW) drag in the context of our sensitivity experiments.

UA-ICON employs the SSO GW drag scheme of Lott and Miller (1997) using its default parameter settings. Figure 1 (adapted from Figure 6 in Mehrdad et al., 2025a, also added as Figure A2a in the revised manuscript) shows the extended-winter (NDJFM) zonal-mean climatology of the SSO-induced zonal-wind tendency together with the zonal-mean wind. Two maxima appear: (i) a primary one in the upper stratosphere and (ii) a secondary maximum in the mid-latitude lower stratosphere, centred slightly below 100 hPa, corresponding to the so-called valve layer (Kruse et al., 2016). This maximum is located on the upper flank of the zonal-mean UTLS jet. A comparable structure appears in other UA-ICON climatologies (e.g., Kunze et al., 2025) using the same scheme and parameters. The precise altitude of this secondary maximum is sensitive to both the local jet structure and to scheme parameters such as the critical Froude and Richardson numbers.

In our simulations, the secondary maximum lies near the lower boundary of the valve layer, somewhat lower than the multi-model mean of CMIP6 AMIP OGWD climatologies reported by Hájková & Šácha (2024), where freely propagating OGWs typically deposit momentum above ≈ 100 hPa. However, their analysis also shows a large inter-model spread in the vertical position of this peak, linked to scheme design and tuning. Thus, the placement in UA-ICON remains physically reasonable and consistent with the broader range found in CMIP6.

Figure 2 (adapted from Figure 3 in Mehrdad et al., 2025a) further illustrates that the vertical structure of SSO drag differs across the EA, NA, and HI hotspot regions. In the control climatology (blue curves), NA and HI exhibit enhanced drag centered below ≈ 100 hPa, whereas EA shows a maximum extending higher into the lower stratosphere. These regional variations arise from differences in GW generated in the SSO scheme and in local jet altitude, both of which control where critical-level saturation occurs. When the forcing is intensified (orange/green/red curves), the vertical distribution responds accordingly—strengthening the existing lower-stratospheric peak over NA and HI but the upper peak over EA, demonstrating the role of the background climatology in constraining the response.

Regarding the possible implications for the Northern Hemisphere stratospheric polar vortex (SPV), Hájková & Šácha (2024) found that stronger SSO GW drag in the valve layer tends to enhance resolved-wave drag (EPFD) in the polar lower stratosphere through refractive-index changes ("amplifying interaction"). However, the inter-model mean zonal-wind differences do not show a robust relationship with either the valve-layer SSO GW drag or EPFD. Consequently, while a slightly lower valve-layer peak in UA-ICON could influence the details of upward wave propagation near the jet, its effect on the climatological SPV strength is expected to be minor within the range of uncertainty documented by CMIP6. A dedicated sensitivity test varying the SSO-scheme parameters would be required to quantify this influence, which lies beyond the present study.

We have added Appendix A (lines 486–506), which provides a concise summary of the spatial and vertical distribution of the imposed SSO-induced zonal wind tendencies by hotspot. We also include the zonal-mean zonal wind tendency climatology of the model control run (Figure A2a of the revised manuscript) and briefly note the lower-stratospheric valve-layer maximum in our UA-ICON simulation. This appendix supplies the essential vertical context without duplicating Mehrdad et al. (2025a).

In addition, we added a paragraph in Section 4.4 (Model limitations and implications) of the revised manuscript (lines 465-472) to explicitly discuss the model's SSO GW drag climatology, its relationship to the valve layer, and how the vertical placement compares with the CMIP6 AMIP multi-model mean reported by Hájková & Šácha (2024).

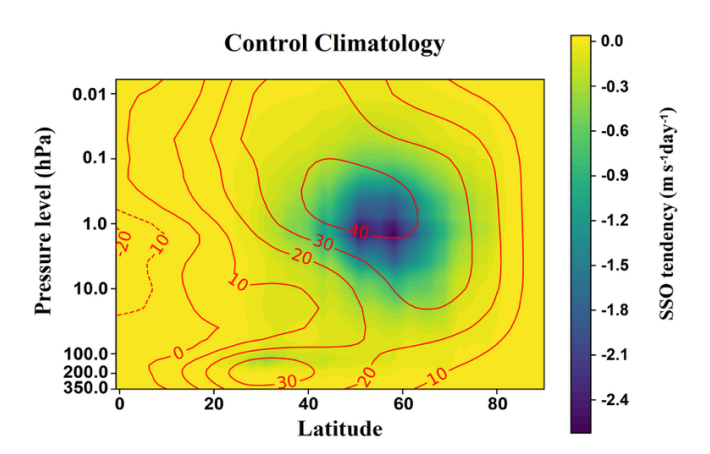


Figure 1: Zonal-mean climatology of the SSO-induced zonal wind tendency (color shading), with red contours indicating the climatology of the zonal-mean zonal wind (m s⁻¹) in the control simulation. The climatologies are computed for the extended winter period (NDJFM). Adapted from Mehrdad et al. (2025a).

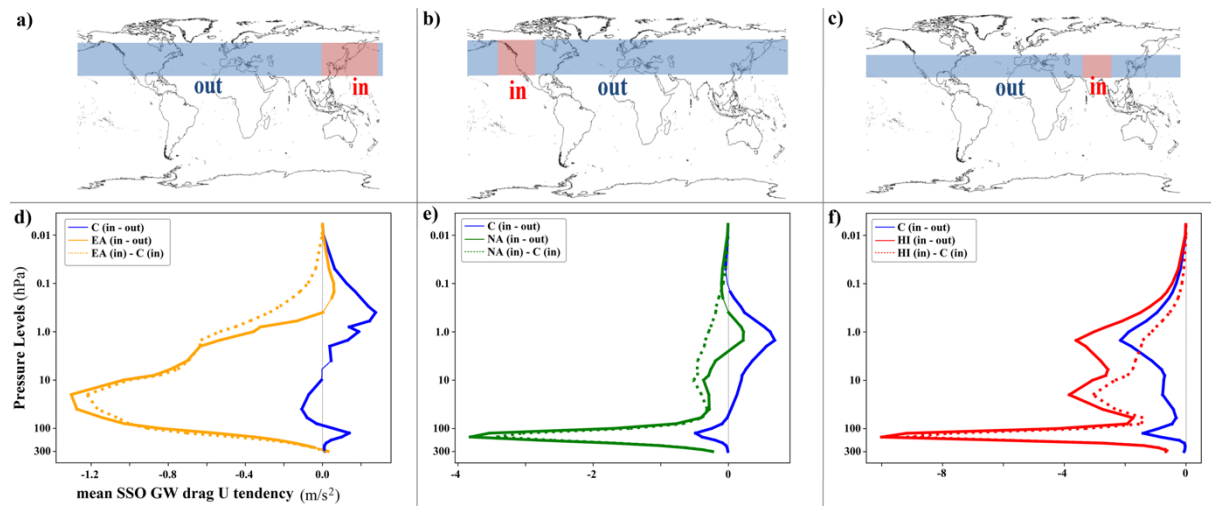


Figure 2: (a–c) Maps showing the latitudinal bands of the forcing regions for the EA (a), NA (b), and HI (c) hotspot. The "in" regions correspond to the areas where the forcing is applied, while the "out" regions represent the same latitude bands outside the hotspot regions. (d–f) Vertical profiles of the SSO-induced zonal wind tendency (m s⁻²) during the extended winter period (NDJFM), calculated from ensemble means. Each column corresponds to one sensitivity simulation: EA (d), NA (e), and HI (f). The solid blue lines show the control run climatology, computed as the difference between the "in" and "out" regions. Solid orange, green, and red lines represent the corresponding differences between "in" and "out" regions in the EA, NA, and HI simulations, respectively. Dashed lines indicate the difference between each sensitivity simulation and the control run for the forced ("in") regions. Thickened line segments denote regions where the differences are consistent.

I miss the motivation why such a methodology has been applied to classify the SPV geometry compared to either standard clustering techniques (e.g. k-means in Kretschmer et al (2018)) and/or standard techniques for split and displacement identification (e.g. Seviour et al, 2013)

Thank you for this helpful suggestion. We have revised Section 2.3 (Classification of SPV geometry) to make the motivation explicit. In brief, previous work has used geometric diagnostics (e.g., centroid latitude, aspect ratio) to identify displaced/split states (Seviour et al., 2013; Mitchell et al., 2013), which is transparent but coarse; or (ii) applied field-based

clustering on dynamical fields (e.g., k-means/hierarchical clustering as in Kretschmer et al., 2018), which offers a holistic view but is sensitive to small spatial shifts/rotations of the vortex. Our revised Section 2.3 explains that we combine the strengths of both by representing the vortex boundary geometry with Fourier descriptors and then clustering in that low-dimensional, physically interpretable feature space. Low-order harmonics quantify circularity/elongation/orientation, higher orders capture finer deformations, and truncation to the leading modes emphasizes large-scale morphology and reduces sensitivity to small-scale noise and minor spatial shifts. This provides a stable, morphology-based classification that is more informative than a handful of scalars yet less shift-sensitive than gridpoint-wise clustering. (See Section 2.3, lines 112-133)

Can you include the value of the 18% threshold mentioned in Section 2.3.1 and Fig. 1?

We thank the reviewer for this comment. The 18% threshold is defined as the 18th percentile of the daily 10 hPa geopotential height (GPH) distribution. We have revised the corresponding sentence in Section 2.3.1 (lines 137-138) to make it clearer.

Due to the extensiveness and unique methodology of the study, I think the whole community would appreciate an adoption of Open Science approaches to allow reproducing the extensive analysis in this study (e.g. Laken, 2016). In particular, I would recommend any kind of willingness of the authors to publish the code or a series of functions allowing to reproduce the figures in the paper. There are multiple ways to proceed, either to allow access upon request or via portals that allow assigning Digital Object Identifier (DOI) to the research outputs, e.g. ZENODO. I think it could enhance the quality and reliability of this publication.

We thank the reviewer for this valuable suggestion. The datasets used in this study are already publicly available via the WDCC. In addition, we now explicitly state in the "Data Availability" section that the analysis code used for the clustering, projection, and wave-diagnostic calculations is available upon request (lines 484-485 of the revised manuscript).

As shown in Mitchell et al (2011), splits are also accompanied by equatorward shift of the vortex (diagnosed by centroid latitude), i.e. a PW1-like pattern. In this view, I would suggest discussing results in Sections 3 and 4. Some studies find little (e.g. Maycock, A. C., and P. Hitchcock, 2015) or strong (e.g. Mitchell e al, 2013) differences between the surface impacts of split and displacement events. Have authors found any surface signatures in the sensitivity experiments?

We thank the reviewer for this helpful suggestion. To clarify the role of PW1 and PW2 in shaping split-vortex states, we have added a sentence on line 526-529 in the revised manuscript in (Appendix D of the revised manuscript).

Although we did not explicitly diagnose centroid latitude, the concurrent PW1 amplitude is qualitatively consistent with Mitchell et al. (2011).

Regarding the surface response, assessing the delayed tropospheric impacts of these stratospheric perturbations lies beyond the scope of the present cluster-based framework, which focuses on the simultaneous upper-stratospheric response. Nevertheless, as shown in Mehrdad et al. (2025a, their Appendix A/Figure A1), all sensitivity experiments display a tendency toward a negative Arctic Oscillation phase following the imposed gravity-wave hotspots, even though the SSW frequency is not significantly different among experiments (see Figure 4 in Mehrdad et al. 2025a). All experiment data are publicly available to facilitate further investigation of stratosphere—troposphere coupling and surface impacts. We consider this an interesting avenue for follow-up analysis and welcome such studies using our dataset.

I had trouble seeing dotted regions and contours in Figs. 3,4,5. I encourage authors to enhance their clarity. The choice of colours (cyan and green) in Fig. 10 could also be improved.

We thank the reviewer for this valuable feedback. In the revised manuscript, Figures 3 and 4 have been modified, and their subplots have been slightly enlarged to improve the visibility of the dotted regions and contours. The former Figure 5 (now Figure C1) is also scaled up. Regarding the cyan and lime contour overlays used, we carefully evaluated alternative colour options. However, these colours offer the best balance: they remain visible against both strong positive and negative anomalies, where darker contour colours tend to become indistinguishable. Although cyan and lime contours are less distinct over near-zero (white) regions, they provide better overall contrast across the full anomaly range. For this reason, we decided to retain these colours in the revised figures.

I would replace abbreviations (EA, HI, NA) with their full length in subsection titles.

We thank the reviewer for this helpful suggestion. The subsection titles have been revised to include the full names, now reading:

Himalayas (HI), Northwest America (NA), and East Asia (EA).

I would move Fig. 5 to the appendix/supplement.

We thank the reviewer for this helpful suggestion. In the revised manuscript, the former Figure 5 has been moved to Appendix C (lines 513–518) and is now labelled as Figure C1. The corresponding descriptive text has also been moved to this appendix. In addition, a reference to Appendix C has been added in Section 3.1 (line 241) to guide the reader to the section.

Have you considered decomposing EPFD into leading zonal planetary wave modes? As shown in Sacha et al (2021), diverse dynamical responses to OGWD hotspots, particularly given the different wavenumbers. This has been in details discussed in Kuchar et al (2022), highlighting that strong and intermittent OGW drag events above the Himalayas in the lower stratosphere are associated with anomalously increased upward RW propagation in the stratosphere. This is somewhat different to the

conclusion of this study. Overall, I suggest discusses differences in findings from previous studies in the manuscript.

Thank you. Yes, we have performed the wavenumber decomposition in our previous paper, Mehrdad et al. (2025a), where the UA-ICON ensemble experiments with regionally enhanced SSO GW drag showed that the resolved response is dominated by PW1, with suppressed upward and equatorward propagation and weakened wave drag overall (see Figures 10–12 in Mehrdad et al., 2025a).

In the present manuscript, we quantify the leading PW modes explicitly in terms of wave amplitude. Figure 4 shows that all three hotspot forcings reduce PW1 amplitudes at 10 hPa, together with a PW1-like displacement of the vortex (and smaller PW2 effects).

Regarding consistency with Šácha et al. (2021) and Kuchar et al. (2022): those studies diagnose short-time-scale, event-composite responses to naturally occurring strong orographic GW drag peaks near the valve layer in a specified-dynamics Canadian Middle Atmosphere Model (CMAM) setup. By contrast, our UA-ICON experiments apply regionally localized intensification of SSO drag and evaluate the NDJFM ensemble-mean response across 180 model years. In that climate-mean framework, the net signal is a hemispheric reduction of PW1 amplitude and weaker resolved wave drag in mid- and high latitudes, i.e., the time-integrated effect of many intermittent events together with background-state adjustments. This reconciles the different conclusions: short-lived event composites can show episodic responses that average out in the long-term response, leaving the dominant PW1 weakening documented here.

To address your suggestion directly, we have (i) clarified in the manuscript that PW1 dominates the response, with a pointer to our earlier study (lines 69-71 in the introduction, lines 246-247 in Section 3.1), and (ii) added a paragraph in the Discussion contrasting our climate-mean setup with the event-based analyses of Šácha (2021) and Kuchar (2022) (section 4.2 Common response to localized GW forcing, lines 376-383).

Technical comments

L315 (Figure 9. -> (Figure 9).

Thanks, The typo has been addressed in the revised manuscript.

References

Hajková, D., Sacha, P. Parameterized orographic gravity wave drag and dynamical effects in CMIP6 models. Clim Dyn 62, 2259–2284 (2024). https://doi.org/10.1007/s00382-023-07021-0

Kretschmer, M., D. Coumou, L. Agel, M. Barlow, E. Tziperman, and J. Cohen, 2018: More-Persistent Weak Stratospheric Polar Vortex States Linked to Cold Extremes. Bull. Amer. Meteor. Soc., 99, 49–60, https://doi.org/10.1175/BAMS-D-16-0259.1.

- Kruse, C. G., Smith, R. B., and Eckermann, S. D.: The midlatitude lower-stratospheric mountain wave "valve layer", Journal of the Atmospheric Sciences, 73, 5081–5100, https://doi.org/10.1175/JAS-D-16-0173.1, 2016.
- Kuchar, A., Sacha, P., Eichinger, R., Jacobi, C., Pisoft, P., and Rieder, H.: On the impact of Himalaya-induced gravity waves on the polar vortex, Rossby wave activity and ozone, EGUsphere [preprint], https://doi.org/10.5194/egusphere-2022-474, 2022.
- Laken, B. A. (2016). Can Open Science save us from a solar-driven monsoon? Journal of Space Weather and Space Climate, 6, A11. http://doi.org/10.1051/swsc/2016005020.
- Maycock, A. C., and P. Hitchcock (2015), Do split and displacement sudden stratospheric warmings have different annular mode signatures?, Geophys. Res. Lett., 42, 10,943–10,951, doi:10.1002/2015GL066754.
- Mehrdad, S., Marjani, S., Handorf, D., and Jacobi, C.: Non-zonal gravity wave forcing of the Northern Hemisphere winter circulation and effects on middle atmosphere dynamics, EGUsphere, 2025, 1–35, https://doi.org/10.5194/egusphere-2025-3005, 2025a.
- Mitchell, D. M., A. J. Charlton-Perez, and L. J. Gray, 2011: Characterizing the Variability and Extremes of the Stratospheric Polar Vortices Using 2D Moment Analysis. J. Atmos. Sci., 68, 1194–1213, https://doi.org/10.1175/2010JAS3555.1.
- Mitchell, D. M., L. J. Gray, J. Anstey, M. P. Baldwin, and A. J. Charlton-Perez, 2013: The Influence of Stratospheric Vortex Displacements and Splits on Surface Climate. J. Climate, 26, 2668–2682, https://doi.org/10.1175/JCLI-D-12-00030.1.
- Sacha, P., Kuchar, A., Eichinger, R., Pisoft, P., Jacobi, C., & Rieder, H. E. (2021). Diverse dynamical response to orographic gravity wave drag hotspots—a zonal mean perspective. Geophysical Research Letters, 48, e2021GL093305. https://doi.org/10.1029/2021GL093305
- Seviour, W. J. M., D. M. Mitchell, and L. J. Gray (2013), A practical method to identify displaced and split stratospheric polar vortex events, Geophys. Res. Lett., 40, 5268-5273 doi:10.1002/grl.50927.